DOI: 10.1002/ange.201209676

Carbon Nanomaterials

Ultralight, Flexible, and Fire-Resistant Carbon Nanofiber Aerogels from Bacterial Cellulose**

*Zhen-Yu Wu, Chao Li, Hai-Wei Liang, Jia-Fu Chen, and Shu-Hong Yu**

Carbon-based aerogels, composed of interconnected three-dimensional (3D) networks, have attracted intensive attention because of their unique physical properties, such as low density, high electrical conductivity, porosity, and specific surface area.[1–3] As a result, carbon-based aerogels are promising materials used as catalyst supports,[4] artificial muscles,[5] electrodes for supercapacitors,[6] absorbents,[7] and gas sensors.[8] Especially, ultralight or flexible carbon-based aerogels have many potential applications. For example, ultralight nitrogen-doped graphene framework, used as an absorbent for organic liquids or the active electrode material, exhibits a high absorption capacity and specific capacitance;[9] stretchable conductors, fabricated by infiltrating flexible graphene foam with elastic polymers, show high stability of electronic conductivity even under high stretching and bending strain.[10]

Traditionally, to fabricate carbon aerogels, resorcinol–formaldehyde organic aerogels were pyrolyzed in an inert atmosphere to form a highly cross-linked carbon structure.[11,12] The carbon aerogels always have a high density (100–800 mg cm^{-3})[11,13] and tend to break under compression. Carbon nanotube (CNT) sponges,[7] graphene foam,[10] and CNT forests[14] have been prepared through chemical vapor deposition (CVD). Meanwhile, CNTs and graphene can be employed as building blocks and assembled into macroscopic 3D architectures.[15–18] However, the harmful and expensive precursors or complex equipments involved in these syntheses dramatically hamper the large-scale production of these carbon-based aerogels for industry application. Recently, we have developed a template-directed hydrothermal carbonization process for synthesis of carbonaceous nanofiber hydrogels/aerogels on macroscopic scale by using glucose as precursors.[19] However, the use of expensive nanowire templates in this synthesis pushes us to explore a facile, economic, and environmentally friendly method to produce carbon-based nanostructured aerogels.

Nowadays, there is a trend to produce carbon-based materials from biomass materials, as they are very cheap, easy to obtain, and nontoxic to humans, etc.[20] Bacterial cellulose (BC), a typical biomass material, is composed of interconnected networks of cellulose nanofibers,[21,22] and can be produced in large amounts in a microbial fermentation process.[22] Recently, we reported a highly conductive and stretchable conductor, fabricated from BC, shows great electromechanical stability under stretching and bending strain.[23]

Herein, we report a facile route to produce ultralight, flexible, and fire-resistant carbon nanofiber (CNF) aerogels in large scale from BC pellicles. When used as absorbents, the CNF aerogels can absorb a wide range of organic solvents and oils with excellent recyclability and selectivity. The absorption capacity can reach up to 310 times the weight of the pristine CNF aerogels. Besides, the electrical conductivity of the CNF aerogel is highly sensitive to the compressive strain, thereby making it a potential pressure-sensing material.

For fabricating the CNF aerogels, a piece of purified BC pellicle with the size of $320 \times 240 \times 12$ mm^3 was first cut into rectangular or cubic shape and then freeze-dried to form BC aerogels (see the Supporting Information). The dried BC aerogels were pyrolyzed at 700–1300 °C under argon atmosphere to generate black and ultralight CNF aerogels. After pyrolysis, the volume of obtained CNF aerogel is only 15 % of that of the original BC aerogel. Meanwhile, the density decreases from 9–10 mg cm^{-3} for BC aerogels to 4–6 mg cm^{-3} for CNF aerogels, owing to evaporation of volatile species. The macroscopic sizes of the as-synthesized CNF aerogels are dependent on the sizes of the BC pellicles cut in the fabrication procedure.

It is well-known that temperature has a great influence on pyrolysis products.[24] To create ideal CNF aerogels, BC aerogels were pyrolyzed separately at different temperatures. Scanning electron microscopy (SEM) images show that BC aerogels exhibit a porous, interconnected, well-organized 3D network structure, which was formed through self-assembly in the bacteria culture process (Figure 1 a). A high-magnification SEM image indicates that the nanofibers with a diameter of 20–80 nm are highly interconnected with large numbers of junctions (see the Supporting Information, Figure S1). After the pyrolysis treatment, the porous 3D structure of BC aerogels was maintained, and the diameter of the nanofibers decreased to 10–20 nm (Figure 1 b, also see the Supporting

[*] Z. Y. Wu, C. Li, Dr. H. W. Liang, Prof. Dr. J. F. Chen, Prof. Dr. S. H. Yu
Division of Nanomaterials and Chemistry, Hefei National Laboratory for Physical Sciences at Microscale, Department of Chemistry, CAS Key Laboratory of Mechanical Behavior and Design of Materials, the National Synchrotron Radiation Laboratory, University of Science and Technology of China
Hefei, Anhui 230026 (P.R. China)
E-mail: shyu@ustc.edu.cn
Homepage: http://staff.ustc.edu.cn/~yulab/

[**] This work is supported by the National Basic Research Program of China (Grant 2010CB934700), the Ministry of Science and Technology of China (Grant 2012BAD32B05-4), the National Natural Science Foundation of China (Grants 91022032, 912271032, 21061160492), the Chinese Academy of Sciences (Grant KJZD-EW-M01-1), the International Science & Technology Cooperation Program of China (Grant 2010DFA41170), the Principal Investigator Award by the National Synchrotron Radiation Laboratory at the University of Science and Technology of China.

Supporting information for this article is available on the WWW under http://dx.doi.org/10.1002/anie.201209676.

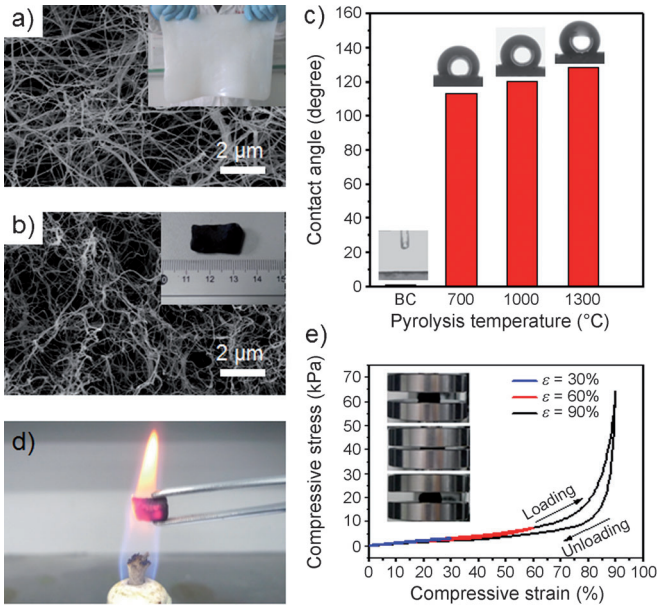

Figure 1. a, b) SEM images of the BC aerogel (a) and the CNF aerogel treated at 1300 °C (b). The insets in (a) and (b) show the photographs of the BC pellicle and the CNF aerogel prepared by pyrolysis at 1300 °C. c) Water contact angle measurements of the original BC aerogel and the CNF aerogels prepared by pyrolysis at different temperatures, indicating that the hydrophobic properties of CNF aerogels improved with increasing pyrolysis temperature. d) Photograph of CNF aerogel in a hot flame of an alcohol burner. e) Compressive stress–strain curves of a CNF aerogel at different set strains ε of 30, 60, and 90%. The inset in (e) shows the sequential photographs of the CNF aerogel during the compression process (in the middle, the compressed form is shown).

Information, Figure S2). No apparent difference in their appearances and morphologies was observed from CNF aerogels generated at different temperatures (see the Supporting Information, Figure S3). The X-ray diffraction (XRD) pattern of original BC showed three characteristic peaks centered at 14.7°, 16.9°, and 22.7°, corresponding to the typical $(1\bar{1}0)$, (110), and (020) planes of cellulose I, respectively[25,26] (see the Supporting Information Figure S4). After pyrolysis at 700 or 1000 °C, these peaks disappeared, thus indicating that the crystalline structure of BC was destroyed during the pyrolysis process and amorphous carbon was formed. When the pyrolysis temperature increased to 1300 °C, a broadened peak centered at 22.4° was observed, corresponding to the (002) plane of graphite.

The effect of pyrolysis temperature was also revealed by Fourier transformed infrared (FTIR) spectra, in which the main absorption peaks of functional groups, such as C=O, C–O, C–H, and -O–H, gradually became weak and finally disappeared, thereby indicating the improvement of carbonization degree with the increase of pyrolysis temperature (see the Supporting Information, Figure S5). The results are further confirmed by X-ray photoelectron spectroscopy (XPS) analysis, in which the atom ratios of C to O are 1.31, 14.13, 17.16, and 20.55 for original BC and the CNF aerogels fabricated at 700, 1000, and 1300 °C, respectively (see the Supporting Information, Figure S6).

A significant change of the surface wettability occurred after pyrolysis treatment (Figure 1c). It was observed that the original BC aerogel exhibits surface superhydrophilicity. When water droplets come into contact with the BC aerogel surface, they spread out completely, exhibiting a low contact angle (< 1°) in the atmosphere. The phenomenon can be explained by the fact that the dried BC aerogel is the product of freeze-dried BC hydrogel, which is superhydrophilic. In contrast, the CNF aerogels became hydrophobic after pyrolysis treatment, and the contact angle of the CNF aerogels changed from 113.50° to 128.64° with increasing pyrolysis temperatures. This result can be explained with FTIR spectra (see the Supporting Information, Figure S5), which show that the number of hydrophilic functional groups, such as C=O, C–O, and -O–H, gradually decreased with increasing pyrolysis temperature; finally these groups disappeared, and the nature of the remaining carbon is hydrophobic. As a result, the CNF aerogel pyrolyzed at 1300 °C has the largest contact angle, which means the best hydrophobic property, and this property promises potential applications in advanced liquid–liquid separation or water treatment technology. Therefore, we chose the CNF aerogels generated from BC pyrolyzed at 1300 °C, which have the highest carbon content and carbonization degree.

The CNF aerogel shown in the inset of Figure 1b has an ultralow density of 4–6 mg cm^{-3}, which is comparable to those of ultralight multiwalled CNT aerogel (4 mg cm^{-3}),[27] CNT sponges (5–10 mg cm^{-3}),[7] and graphene foam grown by CVD (5 mg cm^{-3}),[10] and is only slightly larger than those of the lightest silica aerogels (2–3 mg cm^{-3}) and lightest 3D graphene foam (2.1 ± 0.3 mg cm^{-3}).[9] A piece of CNF aerogel with dimensions of $1.8 \times 0.9 \times 0.7$ cm^3 weighs only 5.6 mg, thus, it can stand on the top of a clover stably (see the Supporting Information, Figure S7). Despite its ultralight property and high porosity (up to ca. 99.7%), CNF aerogel has a high conductivity of 20.6 S m^{-1}, which may find applications in electronic devices. Meanwhile, it exhibits excellent fire-resistance when exposed to the flame of the alcohol burner; the CNF aerogel does not support any burning and remains inert all the time. Even though we repeated this procedure several times, its shape, size, and inherent 3D porous structure remained the same (Figure 1d and Movie S1 in the Supporting Information).

Interestingly, the CNF aerogels display high flexibility that was rarely observed in conventional low-density, high-porosity materials (e.g., silica-based aerogels). The CNF aerogel can bear a manual compression to more than 90% volume reduction and almost recover its original volume after release of the compression, thus showing the aerogel is compliant and elastic. Figure 1e shows plots of compressive stress–strain for the set ε maxima of 30%, 60%, and 90%. Two distinct stages were observed during loading the stress, including a linear elastic region at $\varepsilon < 75\%$, followed by a densification region. In the linear elastic region, the compressive stress gradually increased with the strain, owing to the elastic bending of the nanofibers. In the densification region at $\varepsilon > 75\%$, the stress rises steeply with compression, because the nanofibers impinge upon each other. For all compressive stress–strain tests ($\varepsilon = 30\%$, 60%, and 90%), the unloading curves show

that the stresses remain above zero until $\varepsilon = 0$, thus indicating complete volume recovery without deformations. No obvious changes of CNF morphology in fully recovered aerogels are revealed by SEM images (see the Supporting Information, Figure S8). Although the aerogel was compressed to 90% volume reduction, it had a very low compressive stress of 64 kPa owing to low density and porous structure. The hysteresis loops in all the tests formed by the loading and unloading curves represent typical stress–strain diagrams of elastomeric open cell foams, thereby indicating substantial energy dissipation owing to friction between flowing air and the aerogel skeleton.[7,28] We attribute the robust mechanical properties of the CNF aerogels to both the inherent flexibility of CNFs and the unique interconnected 3D networks of monolithic CNF aerogels.

Owing to their surface hydrophobicity, high porosity, and mechanical stability, the CNF aerogel is an ideal candidate for highly efficient separation/extraction of specific substances, such as organic pollutants and oils. As shown in Figure 2a, when a small piece of CNF aerogel was forced to the gasoline (dyed with Sudan III), it absorbed the oil completely in several seconds, resulting in the clean water originally contaminated by the gasoline. Because of its low density and hydrophobic nature, the CNF aerogel is floating on the water surface after collecting all gasoline, thereby indicating a facile and useful route for cleaning up oil spillage and chemical leakage. The absorption efficiency can be referred to as weight gain, wt%, defined as the weight of absorbed substances per unit weight of pristine CNF aerogel. Various kinds of organic solvents and oils were investigated, such as hydrocarbons (*n*-hexane, cyclohexene, etc.), aromatic compounds (toluene and bromobenzene), and commercial petroleum products (gasoline, diesel oil, and pump oil), which all are common pollutants in daily life or industry. The CNF aerogel exhibits a very high absorption capacity for all of these organic liquids. In general, it can absorb the liquids up to 106 to 312 times its own weight (Figure 2b). The mechanism is mainly physical absorption of organic molecules, which can be stored in the pores of the CNF aerogel. Owing to the low density and high porosity, the absorption efficiency of CNF aerogel is much higher than that of other typical carbon-based absorbents (see the Supporting Information, Table S1), such as spongy graphene (20–86 times),[29] graphene and CNT hybrid foam (80–130 times),[30] CNT sponges (80–180 times),[7] carbonaceous nanofiber aerogel (40–115 times)[19] and even two orders of magnitude higher than that of activated carbon (< 1).[31] To our knowledge, this absorption capacity ranked second among all absorbent materials reported to date for organic solvents and oils; it is only lower than that of the graphene framework (200–600 times), which has a lower density.[9] However, it is difficult to achieve industry application for the graphene framework because of the complicated synthesis procedure and the limited synthetic scale.

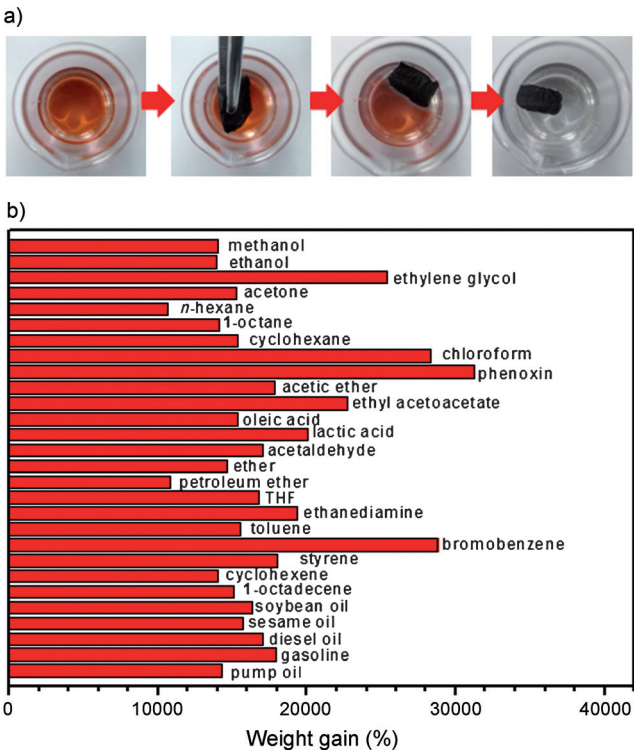

Figure 2. Uptake of organic liquids by the CNF aerogels. a) A layer of gasoline (colored with Sudan III for clear presentation) was absorbed by a CNF aerogel completely in 10 seconds. b) Absorption efficiency of CNF aerogels for various organic liquids.

The recyclability of the CNF aerogels and the recoverability of pollutants are key criteria for oil/chemical cleanup applications. The regeneration of CNF aerogels is illustrated in Figure 3a,b. Direct combustion in air was applied; in this case the absorbed substances are efficiently used for heating. After five absorption/combustion cycles, 124 and 105 times weight gain (89% and 59% for their original absorption capacities) were achieved for ethanol and gasoline, respectively. The absorption capacities decreased with the number of cycles, because the CNF aerogels became smaller during the combustion process. However, the 3D fibrous networks of the CNF aerogel still remained after absorption and combustion, thus making it recyclable for many times. Furthermore, distillation was employed as an alternative method for recycling (Figure 3c,d). After absorption, the sample was heated to the boiling point to release the absorbed liquid. Then, we collected the vapor of the liquid for recycling. No obvious change in absorption capacity was found after five absorption/distillation cycles, because the size and the porosity structure stayed the same during the whole process. The results clearly show the good recyclability of the CNF aerogel when used as an absorbent. Compared with other carbon-based absorbent materials, CNF aerogels have some outstanding features, such as inexpensive and environmentally friendly raw materials, facile preparation, high absorption capacity, good recyclability, and most importantly, the superior ability for large-scale synthesis (see the Supporting Information, Table S1).

Finally, the combined compressible and conductive properties of the CNF aerogels lead to their pressure response. The correlation between electrical resistance of CNF aerogel and compressive strain was investigated (Figure 4a). When the CNF aerogel was gradually compressed, the electrical resist-

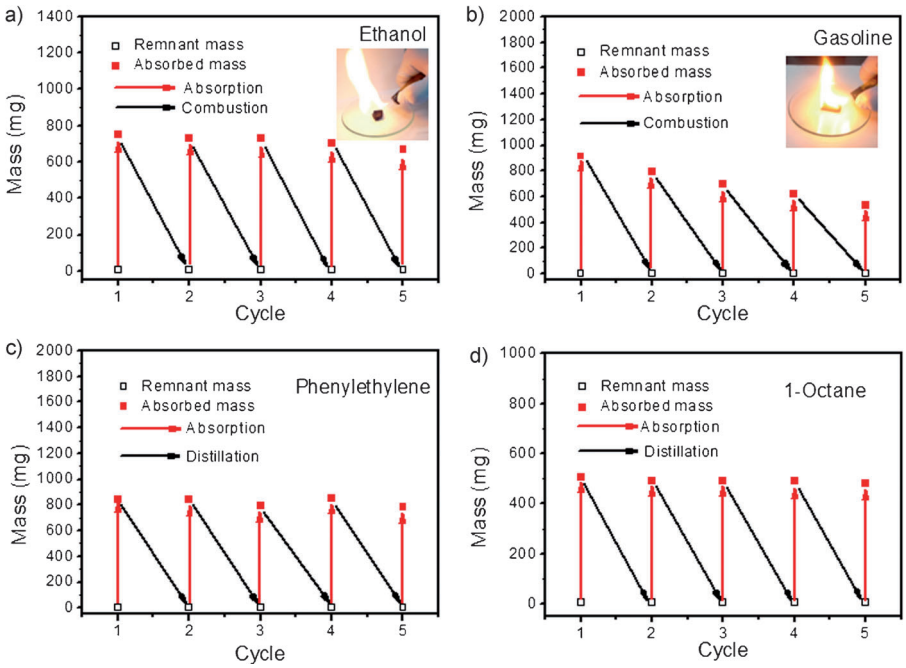

Figure 3. Absorption recyclability of CNF aerogels. a,b) Recyclability of CNF aerogels for absorption of ethanol and gasoline when using the direct combustion method. The insets in (a) and (b) show photographs of burning aerogel saturated with enthanol and gasoline, respectively. c, d) Recyclability of CNF aerogels for absorption of phenylethylene and 1-octane when using the distillation method.

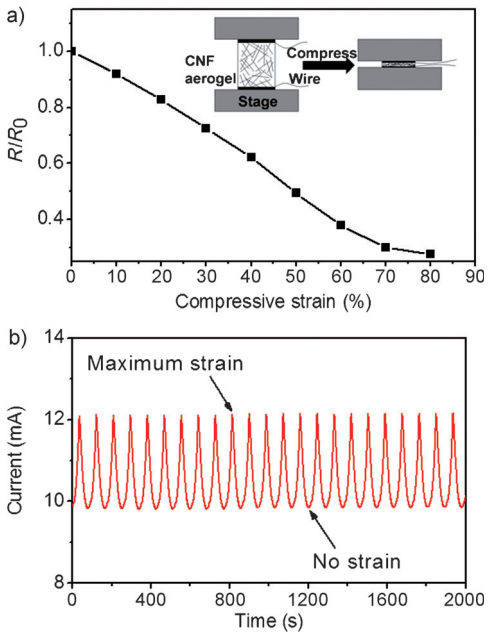

Figure 4. The pressure response of CNF aerogels. a) Plot of the electric resistance variation with compressive strain. The inset in (a) shows an in situ measurement of the electric resistance during the compression process. b) The variation of electric current with cyclic compression in a closed circuit.

ance decreased nearly linearly with the compressive strain ε from 0 to 70%. Interestingly, the results are in accordance with the compressive stress–strain linear elastic region at $\varepsilon <$ 75%. In this region, the interface contact spots of nanofibers and the density of the CNF aerogel increased linearly with the compressive strain, thus leading to electrical resistance decreasing linearly. The decrease of electrical resistance becomes slowly with further increase of compressive strain, because the CNF aerogel has become densified, and only few new interface contact spots were formed during this process. Furthermore, the variation of electric current in a closed circuit was recorded; this experiment shows the continuous change of current with compressive strain and high reversibility of the CNF aerogel as a pressure-sensitive material (Figure 4b).

In conclusion, we report a facile, economic, environmentally friendly method to fabricate the ultralight CNF aerogel with a density of 4–6 mg cm^{-3}. The CNF aerogel has excellent fire-resistant properties, and exhibits extraordinary compressibility. The absorption capability of the BC-derived CNF aerogel can be as high as 106–312 times its own weight for organic pollutants and oils, which is much higher than that of other absorbents. Besides, this kind of CNF aerogel generated from BC can be used for pressure sensors. Other potential applications of the CNF aerogel may include 3D electrode materials for lithium-ion batteries and supercapacitors, catalyst supports, and advanced sensors.

Received: December 4, 2012
Published online: February 10, 2013

Keywords: absorbents · carbon nanofibers · cellulose · nanostructures · pressure sensors

[1] A. C. Pierre, G. M. Pajonk, *Chem. Rev.* **2002**, *102*, 4243.
[2] A. M. ElKhatat, S. A. Al-Muhtaseb, *Adv. Mater.* **2011**, *23*, 2887.
[3] N. Hüsing, U. Schubert, *Angew. Chem.* **1998**, *110*, 22; *Angew. Chem. Int. Ed.* **1998**, *37*, 22.
[4] Z. S. Wu, S. Yang, Y. Sun, K. Parvez, X. Feng, K. Mullen, *J. Am. Chem. Soc.* **2012**, *134*, 9082.
[5] A. E. Aliev, J. Y. Oh, M. E. Kozlov, A. A. Kuznetsov, S. L. Fang, A. F. Fonseca, R. Ovalle, M. D. Lima, M. H. Haque, Y. N. Gartstein, M. Zhang, A. A. Zakhidov, R. H. Baughman, *Science* **2009**, *323*, 1575.
[6] X. C. Dong, H. Xu, X. W. Wang, Y. X. Huang, M. B. Chan-Park, H. Zhang, L. H. Wang, W. Huang, P. Chen, *ACS Nano* **2012**, *6*, 3206.
[7] X. C. Gui, J. Q. Wei, K. L. Wang, A. Y. Cao, H. W. Zhu, Y. Jia, Q. K. Shu, D. H. Wu, *Adv. Mater.* **2010**, *22*, 617.
[8] F. Yavari, Z. P. Chen, A. V. Thomas, W. C. Ren, H. M. Cheng, N. Koratkar, *Sci. Rep.* **2011**, *1*, 166.
[9] Y. Zhao, C. Hu, Y. Hu, H. Cheng, G. Shi, L. Qu, *Angew. Chem.* **2012**, *124*, 11533; *Angew. Chem. Int. Ed.* **2012**, *51*, 11371.

[10] Z. P. Chen, W. C. Ren, L. B. Gao, B. L. Liu, S. F. Pei, H. M. Cheng, *Nat. Mater.* **2011**, *10*, 424.
[11] D. C. Wu, R. W. Fu, S. T. Zhang, M. S. Dresselhaus, G. Dresselhaus, *Carbon* **2004**, *42*, 2033.
[12] R. W. Pekala, *J. Mater. Sci.* **1989**, *24*, 3221.
[13] R. W. Fu, B. Zheng, J. Liu, M. S. Dresselhaus, G. Dresselhaus, J. H. Satcher, T. E. Baumann, *Adv. Funct. Mater.* **2003**, *13*, 558.
[14] M. K. Shin, J. Oh, M. Lima, M. E. Kozlov, S. J. Kim, R. H. Baughman, *Adv. Mater.* **2010**, *22*, 2663.
[15] M. B. Bryning, D. E. Milkie, M. F. Islam, L. A. Hough, J. M. Kikkawa, A. G. Yodh, *Adv. Mater.* **2007**, *19*, 661.
[16] M. A. Worsley, P. J. Pauzauskie, T. Y. Olson, J. Biener, J. H. Satcher, T. F. Baumann, *J. Am. Chem. Soc.* **2010**, *132*, 14067.
[17] H. P. Cong, X. C. Ren, P. Wang, S. H. Yu, *ACS Nano* **2012**, *6*, 2693.
[18] Y. Xu, K. Sheng, C. Li, G. Shi, *ACS Nano* **2010**, *4*, 4324.
[19] H.-W. Liang, Q.-F. Guan, L.-F. Chen, Z. Zhu, W.-J. Zhang, S.-H. Yu, *Angew. Chem.* **2012**, *124*, 5191; *Angew. Chem. Int. Ed.* **2012**, *51*, 5101.
[20] B. Hu, K. Wang, L. Wu, S. H. Yu, M. Antonietti, M. M. Titirici, *Adv. Mater.* **2010**, *22*, 813.
[21] H. Yano, J. Sugiyama, A. N. Nakagaito, M. Nogi, T. Matsuura, M. Hikita, K. Handa, *Adv. Mater.* **2005**, *17*, 153.
[22] M. Iguchi, S. Yamanaka, A. Budhiono, *J. Mater. Sci.* **2000**, *35*, 261.
[23] H. W. Liang, Q. F. Guan, Z. Zhu, L. T. Song, H. B. Yao, X. Lei, S. H. Yu, *NPG Asia Mater.* **2012**, *4*, e19.
[24] A. Demirbaş, *Energy Explor. Exploit.* **2004**, *22*, 411.
[25] S. Y. Oh, D. I. Yoo, Y. Shin, H. C. Kim, H. Y. Kim, Y. S. Chung, W. H. Park, J. H. Youk, *Carbohydr. Res.* **2005**, *340*, 2376.
[26] K. I. Uhlin, R. H. Atalla, N. S. Thompson, *Cellulose* **1995**, *2*, 129.
[27] J. H. Zou, J. H. Liu, A. S. Karakoti, A. Kumar, D. Joung, Q. A. Li, S. I. Khondaker, S. Seal, L. Zhai, *ACS Nano* **2010**, *4*, 7293.
[28] W. Yu, Y. B. Li, Y. P. Zheng, N. Y. Lim, M. H. Lu, J. T. Fan, *Meas. Sci. Technol.* **2006**, *17*, 1785.
[29] H. Bi, X. Xie, K. Yin, Y. Zhou, S. Wan, L. He, F. Xu, F. Banhart, L. Sun, R. S. Ruoff, *Adv. Funct. Mater.* **2012**, *22*, 4421.
[30] X. Dong, J. Chen, Y. Ma, J. Wang, M. B. Chan-Park, X. Liu, L. Wang, W. Huang, P. Chen, *Chem. Commun.* **2012**, *48*, 10660.
[31] M. A. Lillo-Ródenas, D. Cazorla-Amorós, A. Linares-Solano, *Carbon* **2005**, *43*, 1758.

